

Preliminary Results on a Large Acoustic-Stirling ("Pulse Tube") Cooler Designed for 800W at 70K

P. S. Spoor

Chart Industries / Biomedical Division
Troy, NY 12180

ABSTRACT

The emergence of high-power superconducting devices such as fault-current limiters, and demand for on-site liquefaction and storage of cryogenics and fuels such as hydrogen and natural gas, have in turn spurred demand for larger point-of-use cryogenic cooling. This paper describes the development and preliminary testing of a very large acoustic-Stirling ("pulse-tube") cooler driven by a 20 kWe pressure-wave generator (PWG), and featuring a coaxial coldfinger and long transfer line separating the coldfinger and PWG. The coldfinger design and the 'split' configuration readily enable integration into most relevant applications, though they do present unique challenges at this scale. In this paper we will discuss the challenges inherent in building an acoustic cooler at this large scale, some strategies for lowering cost in production, and preliminary test results on the prototype cooler.

This work was sponsored by the U.S. Department of Energy.

INTRODUCTION

Acoustic-Stirling (or 'pulse-tube') coolers are well-adapted to the rigors of superconducting power applications, due to their intrinsic high efficiency, long life, and maintenance-free operation. Historically, however, 'pulse tube' coolers have had relatively low capacity compared to HTS power system requirements. As the cooling powers of 'pulse-tubes' have increased by orders of magnitude over the last couple decades, from several watts to hundreds of watts, the end users developing superconducting devices have continually sought higher and higher capacities, as well as lower cooling temperatures. The U.S. Department of Energy has provided valuable investment and leadership in this area, by funding the development of larger acoustic cryocoolers, such as our 2S362K-FAR. The development is proceeding in several stages; first, a coldfinger optimized for 70K, and a second coldfinger optimized for 50K (both single-stage). In parallel, we are developing a lower-cost pressure-wave generator (PWG) for driving these coldfingers. Cost is the single biggest challenge in bringing acoustic-Stirling technology to the wider marketplace, as there are few existing mass-produced components that can be leveraged (unlike Gifford-McMahon cryocoolers, which use essentially the same compressor technology as do domestic refrigerators).

One exception is stainless-steel filter material, which is made commercially in porosities and fiber sizes that are well-suited to use in single-stage Stirling-cycle cryocooler regenerators. The traditional material for cryocooler regenerators is fine-mesh stainless-steel woven screen, but in

the quantities required for a 1000W@80K coldfinger, this material is prohibitively expensive and difficult to handle. Our '362' class coldfinger requires about 1500 regenerator elements, if filled with all 400 mesh/inch by 0.0009 inch wire diameter screen, and at least 50 square meters of raw material (or over 500 square feet). By contrast, filling the same regenerator with random-fiber filter elements requires only 84 separate pieces, and the total cost is at least 10 times less than the woven screen.

We have used random-fiber materials with success in smaller single-stage coldfingers, and if the part tolerances are properly controlled (so that there is no leakage past the regenerator on either the inner nor the outer diameter of the regenerator annulus) there is virtually no difference between the optimized performance of small coldfingers (capacities of 10 to 25 W at 80K) using woven screen and using random-fiber filter material. We have yet to demonstrate them with success on a large coldfinger, however. Partly for this reason, we chose to make our first '362-class' coldfinger modular, with flanged joints on both the warm and the cold end, so we could vary the cold end geometry and the regenerator material.

CHALLENGES OF LARGE-SCALE COLDFINGER CONSTRUCTION

Power Density

In general, the characteristic length of a Stirling-cycle coldfinger is fixed by the working gas type, the frequency, and the temperature range. Since all of these tend to be about the same for small coldfingers as for large ones, the tendency is for large coldfingers to increase in diameter much more than in length. This aspect-ratio shift produces all sorts of secondary mechanical challenges; for instance, if the actual cold-tip is made of copper, brazed to a stainless housing, the large-diameter annealed copper coldtip has a much greater tendency to distend under pressure than a small-diameter coldtip, unless the coldtip is made longer as a fraction of the overall coldfinger length. Thus the mass of the coldfinger can become very significant.

Hence, there is significant motivation during the design phase to keep the aspect ratio L/d from getting too small. As a result, large coldfingers tend to have a much higher power density than do small coldfingers, and high heat-transfer effectiveness is required, especially on the warm (heat rejection) end. As a point of comparison, our '102' class coldfinger, with about 10W capacity at 80K, has a coldfinger working-gas volume of about 57 cc, which equals 0.18 cold watts per cc. The 362 coldfinger, by contrast, is designed for 1000 W at 80K, and has about 2800cc of working gas volume, or 0.36 cold watts per cc—twice the fundamental power density. In addition to larger and more concentrated heat flows, this tends to make the acoustic intensity higher in these large coldfingers as compared to small ones. Since acoustic power is the dot product of oscillating pressure and flow, a higher power density implies a higher acoustic amplitude.

Secondary Flows

The wider aspect ratio and the higher acoustic amplitude imply a greater susceptibility to secondary flows, i.e., convection cells driven by cyclic flow asymmetries or nonuniform flow distribution in relatively wide, short porous elements. Figure 1 illustrates the notion that when the flow "turns the corner" in a large coaxial coldfinger, it will be harder to guarantee uniformity of the flow as it enters the buffer tube (compared to a smaller coldfinger). If the flow distribution is a function of flow direction, i.e. if the flow is more evenly distributed when flowing back out of the cold end of the buffer tube toward the cold HX, the cyclical asymmetry will encourage the formation of a convection cell in the buffer tube, hurting performance.

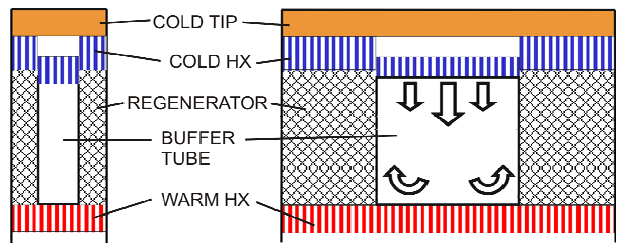


Figure 1. Illustration of nonuniform flow in a coldfinger with small L/d .

Spatially nonuniform temperature may also develop in a large coldfinger, due to secondary flows in the regenerator, for instance. Since the local temperature determines the local gas properties, a temperature nonuniformity across the regenerator may become self-reinforcing. For the same driving pressure wave, a lower cold temperature draws more acoustic power, so more power may be diverted to the already cold regions, driving them even colder and allowing the neighboring regions to warm.

2S362K-FAR EXPERIMENTAL HARDWARE

To mitigate these effects, and to validate the use of low-cost regenerator material, our first test system is constructed in a very modular fashion, to allow swapping of regenerator material or cold-end parts. For example, we have constructed ‘turning vanes’ to guide the flow in the cold plenum between the cold heat exchanger and the cold flow straightener; these vanes are removable, so we can test the performance with and without the vanes. For another, we have fine copper screens and perforated annular copper discs that we can insert into the regenerator matrix at discrete intervals, to “isothermalize” the regenerator and keep temperature within the regenerator radially and azimuthally uniform.

Basic Cryocooler Components

Figure 2 shows the basic components of the 2S362K-FAR cryocooler. The coldhead is mounted on the end of long, flexible transfer line, (the so-called “Flexibly Attached Remote” or FAR line) for better adaptation to various cooling applications.

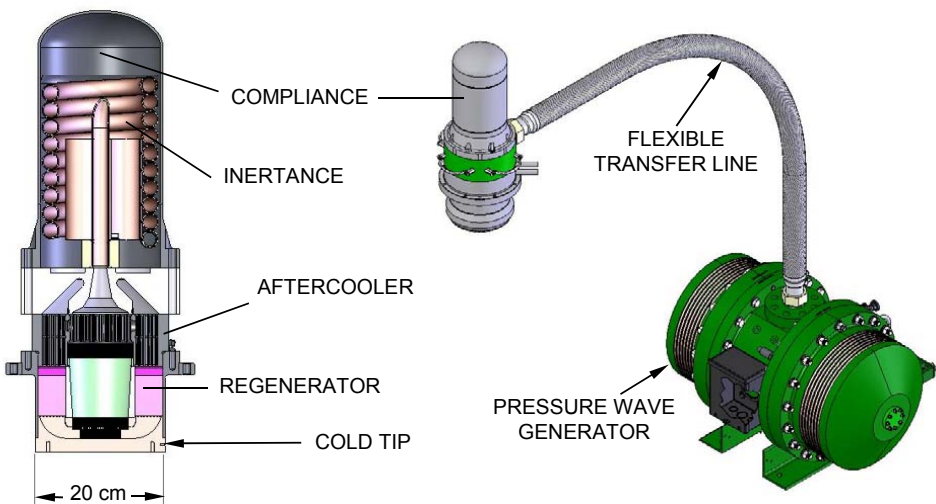


Figure 2. Major components of 2S362K-FAR cryocooler

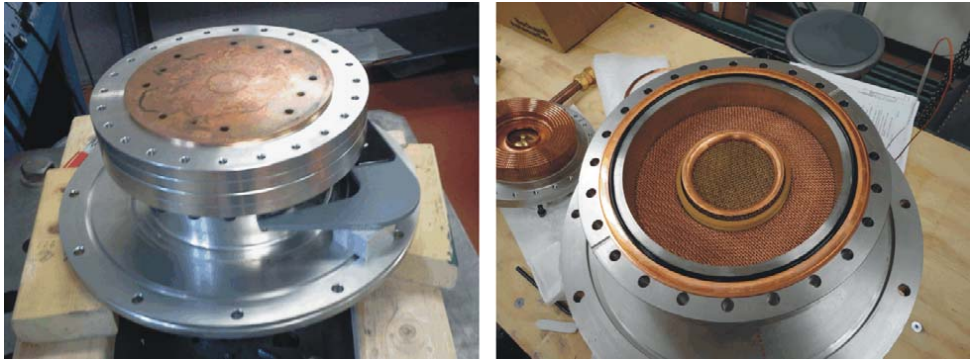


Figure 3. Test version of ‘362’ class coldfinger with cold flange on and off.

In addition to its primary functions of adaptability and vibration isolation, the FAR line has two other important functions. First, due to wavelength effects, the pressure wave amplitude in the pressure wave generator (PWG) is considerably lower than at the coldhead. This reduces the risk associated with the PWG at high acoustic amplitude (i.e. enhanced piston drift, etc.). It also makes the coldhead itself easy to remove, important during this experimental stage.

The coldfinger itself consists of a shell-and-tube aftercooler, a woven-screen regenerator (for the first tests), an integrated sawed-slot copper cold tip, sintered coarse bronze screen flow straighteners, a phenolic (Garolite XX) buffer tube, and an integrated inertance tube and compliance tank. The solid model shown in Figure 2 represents something close to the preferred embodiment of a product (or OEM system); for our initial testing, the transfer line is a simple solid tube and the coldhead itself is modular, with both the cold and warm ends flanged. This flanged coldfinger can be seen in Figure 3. The cold end flange is actually a CF flange, using a copper gasket just like in vacuum systems. Figure 3 shows the flanged coldfinger with and without the flange (the flange is integrated with the sawed-slot heat exchanger). In the right-hand photo, the CF gasket is clearly visible as the band of material just inside the bolt circle. We have used this type of flange successfully on smaller-sized coldfingers, but as will be discussed below, it is much less successful here. In fact, it was *almost* successful, which has caused us to spend more time than we ought trying to make it work.

Figure 4 shows the test setup, with the solid transfer line, and an external inertance tube and compliance tank (so inertance length can be easily changed during optimization) and instrumentation. Our plan was to exercise the cryocooler at $\frac{1}{2}$ power (around 10 kWe of input electric power) to establish successful performance at low amplitude first. That way, if performance shortfalls are observed at high amplitude, we will know to look for amplitude-driven pathologies.

PRELIMINARY RESULTS

Figure 5 shows what actually happened when we started cooling the system down. At very modest cold temperatures, the CF flange began leaking. Even at quarter-power, where the cooling rate is relatively slow, the thermal stresses are still too much. The vacuum, which must remain below ~ 100 mTorr to prevent convective heat leak in the vacuum can, quickly climbs far above this threshold value. Eventually, the pressure inside the can gets large enough that the safety valve pops; the leak is strong enough that despite the large volume of the system, the pressure can be seen to drop slowly. The steady stream of helium flowing through the coldfinger itself is a sizable heat leak, in the form of a steady mass streaming that carries enthalpy from the warm end to the cold end. Unlike conduction or radiation heating, this heat leak is amplitude sensitive and very inconsistent, so one cannot gather useful data in its presence.

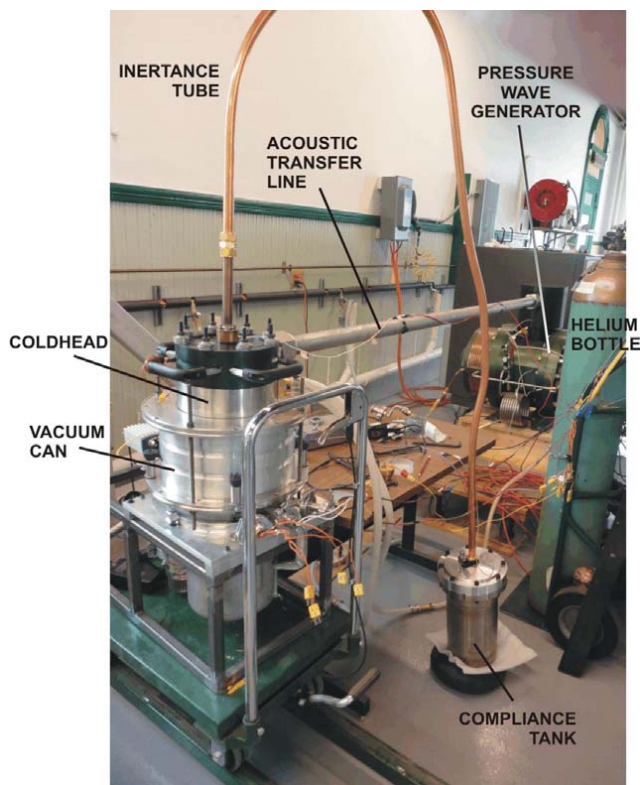


Figure 4. The 2S362K-FAR cryocooler in preliminary testing. Note helium bottle for scale

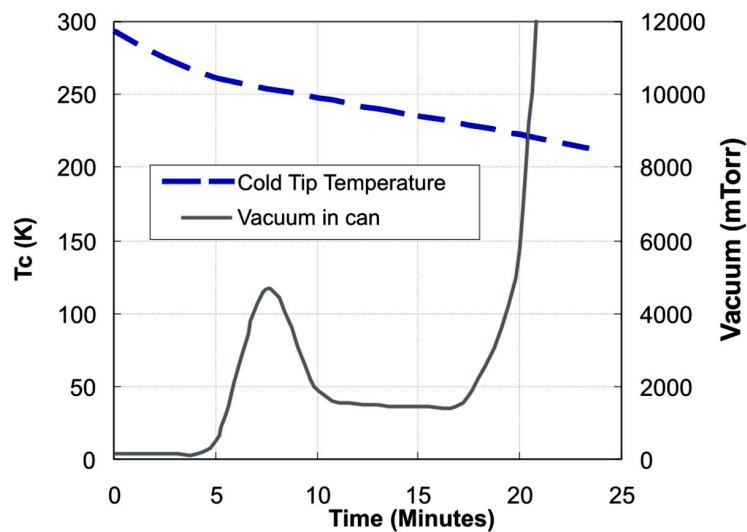


Figure 5. Failure of vacuum in vacuum can during cooldown, running at ¼ power (5 kWe).

At first it was thought to be a mere mismatch between the fasteners and the flanges. Alloy steel bolts were used to compress the stainless-steel flanges, and as alloy steel has a lower coefficient of thermal expansion, the bolts naturally become loose as the coldtip cools. Replacing the alloy bolts with stainless bolts, together with Bellville washers to maintain compression, allowed us to achieve good, strong vacuum for one test session, where we were able to collect a handful of points. Never again have we been able to achieve a good vacuum in the system, suggesting a different approach is needed.

Analysis of available data

We were able to obtain a handful of good-quality data on the cryocooler in its initial configuration (woven screen regenerator, intermittent copper screens for isothermalization, turning vanes in cold plenum) and at low amplitude only (mostly at ¼ power or 5 kWe input). From these data, we were able to form a picture of the cryocooler as basically healthy at low amplitudes. Figure 6 shows a two-point ‘load curve’ of the cryocooler at 5 kWe input; if we assume the curve is linear, we can conclude that the ultimate temperature of this cryocooler is about 50 K, at only ¼ power. For a single-stage cooler, this is a very encouraging result.

Figure 7 shows an attempt to extrapolate the performance at 5 kWe and 77K to higher input powers, to evaluate the absolute performance at 5 kWe as a fraction of full-power performance. In order to do this properly, we need to know the amount of heat leak at 77K. In the absence of internal streaming losses, etc., the heat leak consists of conduction down the regenerator vessel wall, and radiation absorbed by the cold surfaces. Both of these are independent of amplitude, depending only on temperature. The heat leak can be measured by turning off the power to the cryocooler and observing how quickly the temperature rises, then repeating that measurement with a known amount of heat applied to the coldtip. The slopes of the two warmup curves near the target temperature will reveal the baseline heat leak in watts. Our measurement show that the baseline heat leak for this coldfinger is 97 watts at $T_C = 77\text{K}$, $T_H = 300\text{K}$.

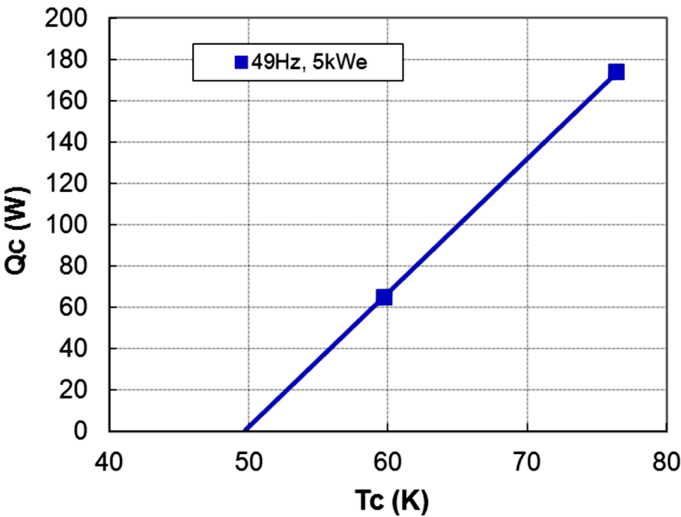


Figure 6. A two-point ‘load curve’ for the 2S362K-FAR at 5 kWe input.

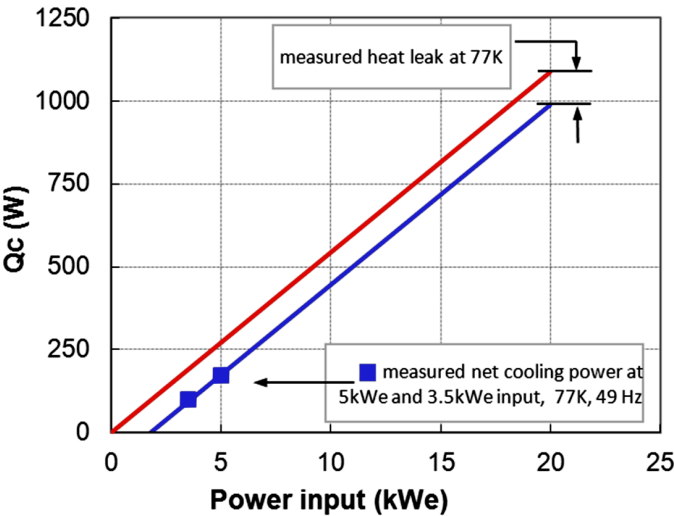


Figure 7. Cooling capacity at low power, extrapolated to high power.

We can define the ‘gross cooling’ of the cryocooler as the applied heat load plus the measured heat leak. We can further assume that the gross cooling scales with power; that is, at 4 times the input power the gross cooling power should be four times greater (if everything is healthy, no harmful secondary flows). If the heat leak remains the same at all powers, then we can estimate the likely net cooling at full power (20 kW) by multiplying the gross cooling at 5 kW input by four, then subtracting the (constant) heat leak.

Figure 7 shows the results. The extrapolated curve suggests that based on our low-power performance, we should expect about 1000 watts of net cooling at 77K, for 20 kW input. As further corroboration, we have added an even lower-power point to the curve, which appears to lie on the same extrapolated line. This is very good evidence that the cryocooler is healthy at low amplitudes, though of course it does not tell us if the performance will still be strong at high amplitudes.

A similar extrapolation for the performance right at 70K, by interpolating the low-power cooling capacity at 70K from Figure 6, indicates that the net cooling at full power is estimated to be 826 watts. This is in excellent accordance with the performance target of 800 W at 70K.

CONCLUSIONS

In general, this is an encouraging beginning to our 2S362K testing. It is very clear that the CF flange does not work well as a make-and-break cold joint at this scale, and we will probably have to resort to an indium O-ring instead (as a backup backup plan, we can weld the flanges together, cut them apart and reweld them at least once).

ACKNOWLEDGMENT

We thank the U.S. Department of Energy for their generous support of this work.

